ISSN No:-2456-2165

Reservoir and Structural Analysis Through Modeling using Well Logs and 3D Seismic Data in OY-1 Field, Onshore Niger Delta, Nigeria

James Abisoye Oyelayo[1]
Daniel Oluwaseun Akinyemi[2]
The Federal University of Technology Akure, Nigeria

Abstract:- This research is centered around employing 3D static modeling, utilizing 3-D seismic and well-log data, to assess the petrophysical characteristics of reservoirs within a Niger Delta field. The primary aim is to determine the extent of movable hydrocarbon resources present within these reservoirs. The seismic data, available in SEG-Y format, played a pivotal role in velocity analysis and structural modeling within the field. Sequential Gaussian simulation and sequential random function simulation techniques were instrumental in achieving this. The integration of these findings with wire-line log data allowed for the extraction of crucial petrophysical attributes like net-to-gross ratio, porosity, water saturation, permeability, and facies distribution. The structural model of the reservoir reveals the presence of distinct listric normal faults named F1 and F2, each displaying unique orientations. The generation of synthetic seismograms facilitated the alignment of well data with seismic data, leading to the identification of four hydrocarbon-bearing sands, labeled as J1, J2, J3, and J4. Among these, the J1 reservoir demonstrates a moderate to good reservoir quality, characterized by commendable porosity (20%), notable permeability (1803Md), moderate net-to-gross ratio (11%), and relatively low water saturation (37%), when compared to J2, J3, and J4. Within the well, the net pay varies between 57 and 209 feet, with J1 exhibiting the highest potential due to its substantial net pay of approximately 209 feet, coupled with the most substantial hydrocarbon movable index, which stands at around 45%.

Keywords:- *Porosity, Permeability, Water Saturation and Fault.*

I. INTRODUCTION

Reservoir modeling entails the creation of a computerized representation of a petroleum reservoir, aimed at facilitating tasks such as assessing hydrocarbon movable index, estimating reserves, devising field development strategies, predicting future production trends, optimizing well placement, exploring alternatives, and managing reservoir resources. The model comprises a 3D grid of discrete cells, each endowed with attributes such as porosity, net-to-gross ratio (NTG), permeability, water saturation, and facies. While geological models provide static depictions of the reservoir within a field, dynamic models utilize finite difference methods to simulate fluid flow during production. In the context of Nigeria, the Niger Delta province stands as a geologically significant region harboring substantial reserves of oil and gas. This province encompasses the Tertiary Niger Delta Akata and Agbada Petroleum System, primarily situated within Nigeria's borders and potentially extending into Cameroon and Equatorial Guinea. Creating a geological reservoir model, such as that for the JA-1 well in OY-Field, involves an intricate description of the reservoir using available data. This encompasses well logs like Density, Gamma-ray, Sonic, and Resistivity log data, in addition to 3D Seismic data. Notably, the absence of Neutron log data in this study presents a challenge in distinguishing between oil and gas reservoirs. The construction of the spatial representative earth model is a key component, followed by its application to flow simulators for forecasting reservoir performance. The objective of this study extends beyond merely aligning the model with current data; it strives to create a model capable of effectively predicting future reservoir behavior, as discussed by Adiela, U.P (2016). In this study, a static modeling approach is adopted for the characterization of the OY-Field reservoir. Integrating static data is a practical yet demanding endeavor, given the diverse data sources originating from various data-collection techniques that contribute to the reservoir modeling process.

- *Study Area Location*

OY-Field is located in the onshore depobelt of the Niger Delta Basin (Figure 2), in which a thick Late Cenozoic clastic sequence of Agbada Formation was deposited in a deltaic fluviomarine environment.

ISSN No:-2456-2165

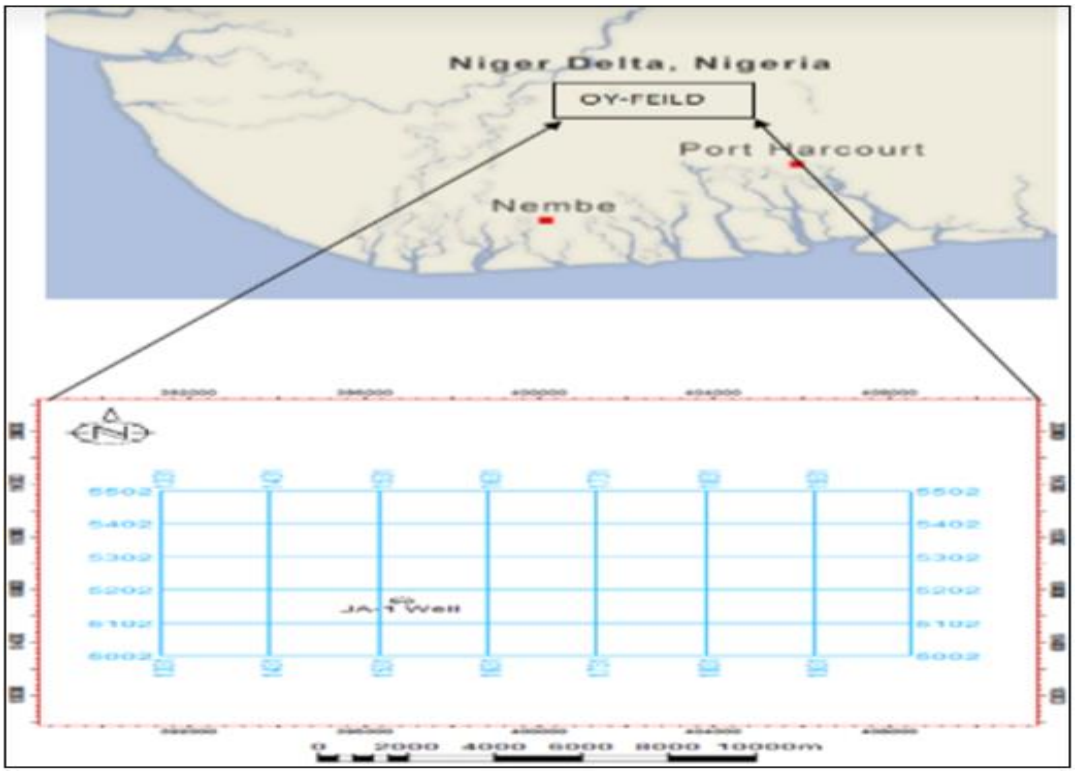

Fig 1 Study Area Location

➢ *Geological setting of the Niger-Delta*

The Niger Delta occupies a geographical space between latitudes 3˚N - 6˚N and longitudes 5˚E - 8˚E in the Gulf of Guinea. Encompassing both onshore and offshore regions of Nigeria, the Niger Delta Basin spans approximately 75,000 square kilometers. Characterized by a regressive clastic sequence, the basin boasts an average maximum thickness of 12,000 meters (39,400 feet). The Niger Delta is partitioned into three formations that delineate distinct depositional facies primarily based on sand-to-shale ratios. At the base of the delta lies the Akata Formation, originating from marine processes. It comprises a substantial shale sequence (a potential source rock), interspersed with turbidite sands (potential deep-water reservoirs), along with minor proportions of clay and silt. The sand content within this layer generally remains under 30%. The Akata Formation was formed from the Paleocene to the Recent era, during times of low sea levels marked by the transportation of terrestrial organic matter and clays to oxygen-deficient (Stacher, 1995), deep-water regions. Above this, the Agbada Formation, the most prominent petroleum-bearing layer, has been forming since the Eocene and continues to develop. Comprising paralic siliciclastic, this formation extends over 3,700 meters in thickness and represents the deltaic segment of the sequence. Here, sand percentages range from 30 to 70%. Deposition occurred across delta-front, delta-topset, and fluvial-deltaic environments. The third formation, the Benin Formation, overlying the Agbada Formation, constitutes a continental deposit from the late Eocene to the Recent period. It is characterized by alluvial and upper coastal plain sands that can reach a thickness of up to 2,000 meters (Avbovbo, 1978). Over the span of around 38 million years, this series of geological events has recurred approximately five to six times, shaping several depobelts within the Niger Delta. These depobelts include the Northern Delta, Greater Ughelli, Central Swamp, Coastal Swamp, and Offshore regions (Figure 1). The escalator regression model, proposed by Knox and Omatsola (1989), depicts the step-wise outward growth of the Niger Delta over geological time. Each step, or depobelt, represents a phase of delta expansion. Depobelts consist of sedimentary bands measuring around 30–60 km in width and up to 300 km in length according to Doust H. and E. Omatsola 1990, delimited by litho-facies variations, counter-regional growth faults, succeeding depo belt's major boundary faults, or combinations thereof at their proximal end, and a significant boundary growth fault at their distal end. Subsequent depobelts contain sedimentary fills noticeably younger than those adjacent in a landward direction. An apparent relationship exists between successive depobelts on a delta dip section. The base alluvial sand facies of an up-dip (older) depobelt align approximately with the initiation of the base sand/shale sequence in the down-dip depobelt. Parallic sequences' deposition within any depobelts concludes with the rapid advancement of alluvial sand facies over proximal and central areas of the belt, initiating the operation of paralic sand/shale sequences in succeeding depobelts.

ISSN No:-2456-2165

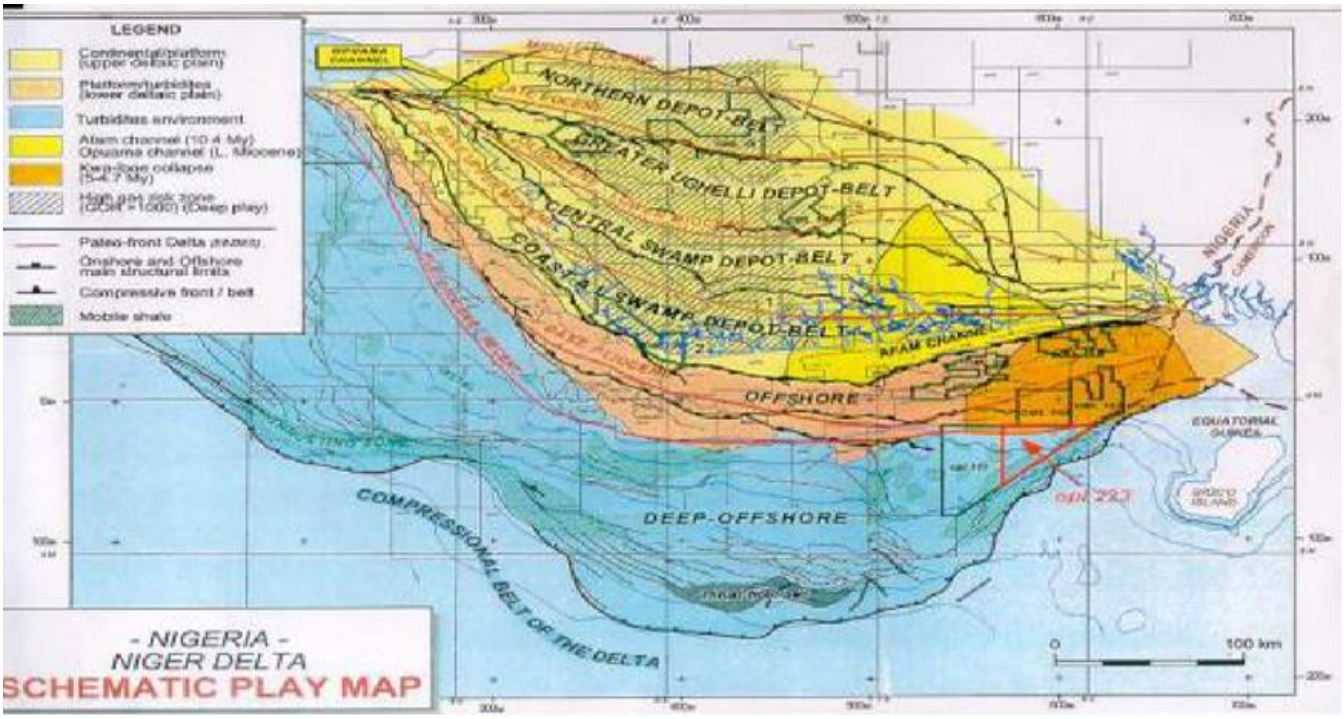

Fig 2 Map of Niger Delta showing the depobelts. (After USGS)

➢ *Aim and Objective*

The aim of this study is to integrate well log and seismic data to generate information that will enable the delineation and estimation of the total volume of hydrocarbon movable index in them. The study also interprets the depositional system on the well logs.

- *The Particular Objectives of the Study are to:*

perform a basic petrophysical evaluation of identified hydrocarbon-bearing sands, generate and interpret time and depth structure maps of key reservoirs, determine and utilize viable direct hydrocarbon indicators in the study area to find new prospects, interpret depositional systems on the good logs, carry out static modeling of the hydrocarbon-bearing reservoirs in the field areas and identified new prospects; and make recommendations for future exploration and production activities in the study area.

II. MATERIAL AND METHODOLOGY

The dataset employed in this study was sourced from a Nigerian oil company. The provided dataset encompassed 3D seismic data, check-shot information, and well-log data. However, it's worth noting that the Neutron log data, which holds the potential to assist in distinguishing between oil and gas in the hydrocarbon-bearing sands of the JA-1 well within the OY field, was not included, posing a challenge in this aspect. The first step in data interpretation is to check the quality of the dataset to be used for interpretation. The dataset employed for this study comprises both 3D seismic data and well-log information. The log data provided were in LAS format also the 3D seismic data were in SEGY format. The bin spacing of the data is 25 by 25 methods and the record length is 6.0sThe data exhibits commendable reflection quality, with clear discernibility of fault and stratigraphic picks for horizons. The well-log analysis was predominantly concentrated within the region covered by well logs. Notably, the JA-1 Well, which served as the focus of this study, was drilled to a depth of 12,230 feet.

A. Materials

➢ *Base Map*

Following the integration of diverse data types, a foundational map (illustrated in Figure 3) for the study area was formulated. The base map was not supplied with the data but was generated using the Schlumberger Petrel™ software.

➢ *Geophysical Well Log*

Well, logs data include the well heads and suite of logs. The logs available are as shown (Table 1).

➢ *Seismic Data*

The seismic data used for this research was in SEG-Y format. It has 688 inlines and 501 crosslines.

➢ *Checkshot*

The checkshot contains two-way travel time and depth which was used for seismic-to-well tie and generation of time-depth relationship curve for conversion of time structural maps to depth equivalents.

➢ *Software*

The data analysis, interpretation, and modeling procedures described in this document were conducted utilizing Schlumberger's PetrelTM2015 software platform in conjunction with Microsoft Excel. PetrelTM is specifically designed to facilitate a seamless "seismic to simulation" workflow, encompassing functions such as data visualization, interpretation, and the integration of information to construct simulation models..

ISSN No:-2456-2165

B. Method of Study

➢ *The Workflow for this Project is shown in (Figure 4).*

- *Qualitative Log Interpretation*

This interpretation technique involves visual inspection of the log signature to obtain information on log trend, log motive, and fluid type. The qualitative interpretation was done in this project work under the listed operations:

✓ *Lithology Interpretation*

A Gamma-ray (GR) log was employed to demarcate the lithology, particularly the presence of sand and shale bodies, within the study area. The traditional GR log was calibrated to a range of 0-150 API, with a designated threshold of 70 API. In this context, readings exceeding 70 API indicated a high radioactive content, while values below this threshold pointed to a lower radioactive content. Identification of sand bodies was achieved through the leftward deflection on the GR log, attributed to diminished radioactive material concentrations. Conversely, shale was discerned by a rightward deflection, indicative of heightened radioactive mineral concentrations. This phenomenon is illustrated in (Figure 5).

✓ *Reservoir Delineation*

Hydrocarbon-bearing reservoirs were discerned through qualitative analysis utilizing a resistivity log, a crucial fluid identification instrument. By integrating the resistivity log with the GR log, the distinction between hydrocarbon and non-hydrocarbon bearing zones was established. Specifically, within hydrocarbon-bearing formations, the resistivity log exhibited notably higher resistivity values compared to water-bearing formations. This distinction is visually illustrated in (Figure 6).

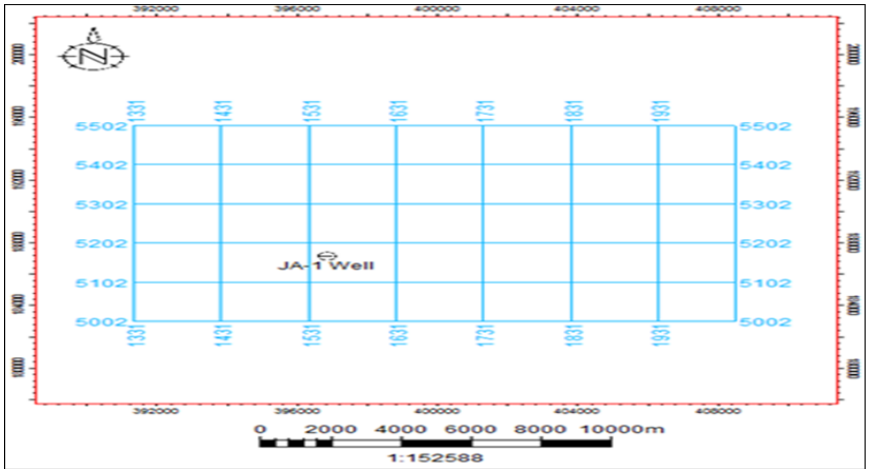

Fig 3 Base Map

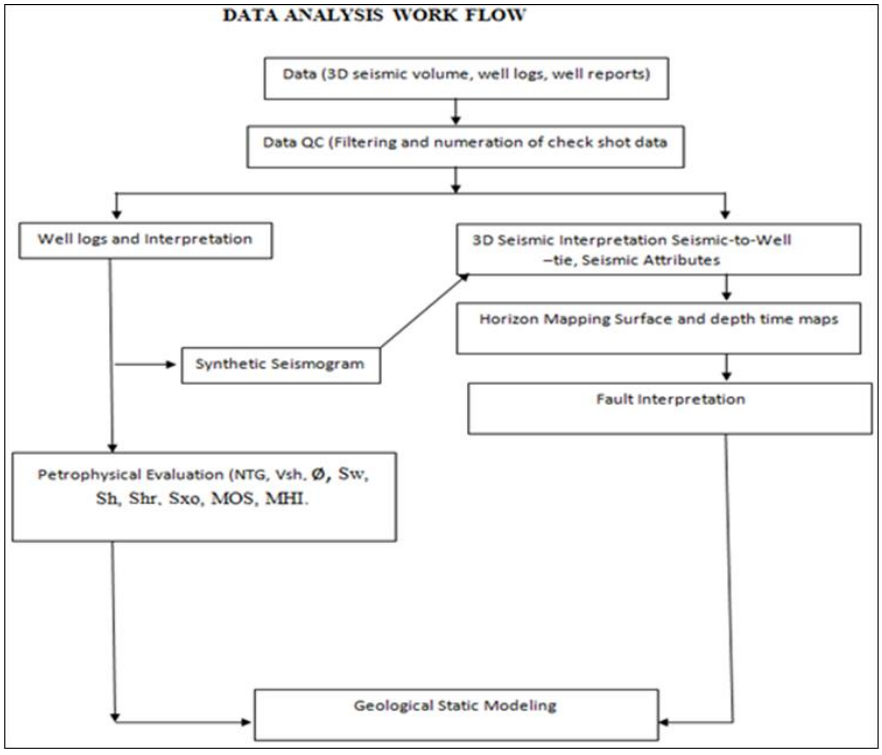

Fig 4 Workflow

ISSN No:-2456-2165

Table 1 Well logs

Logs	JA-1 Well
Gamma ray	•
Density	•
Resistivity	•
Neutron	×
Sonic	•

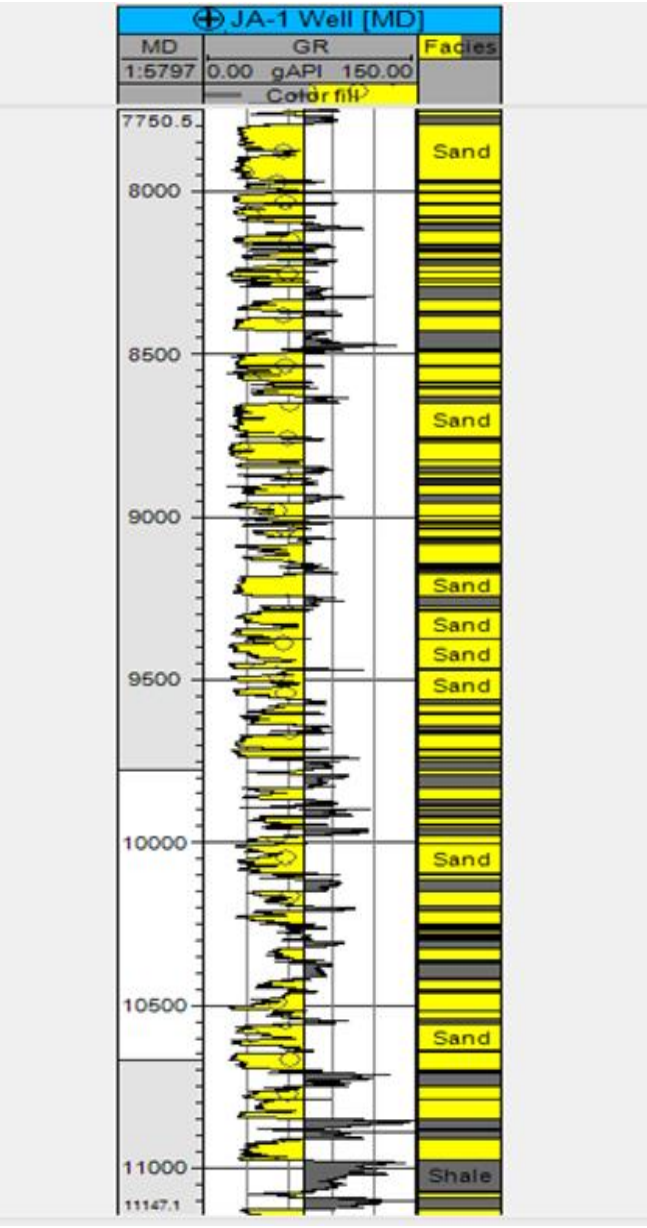

Fig 5 Lithology Interpretation

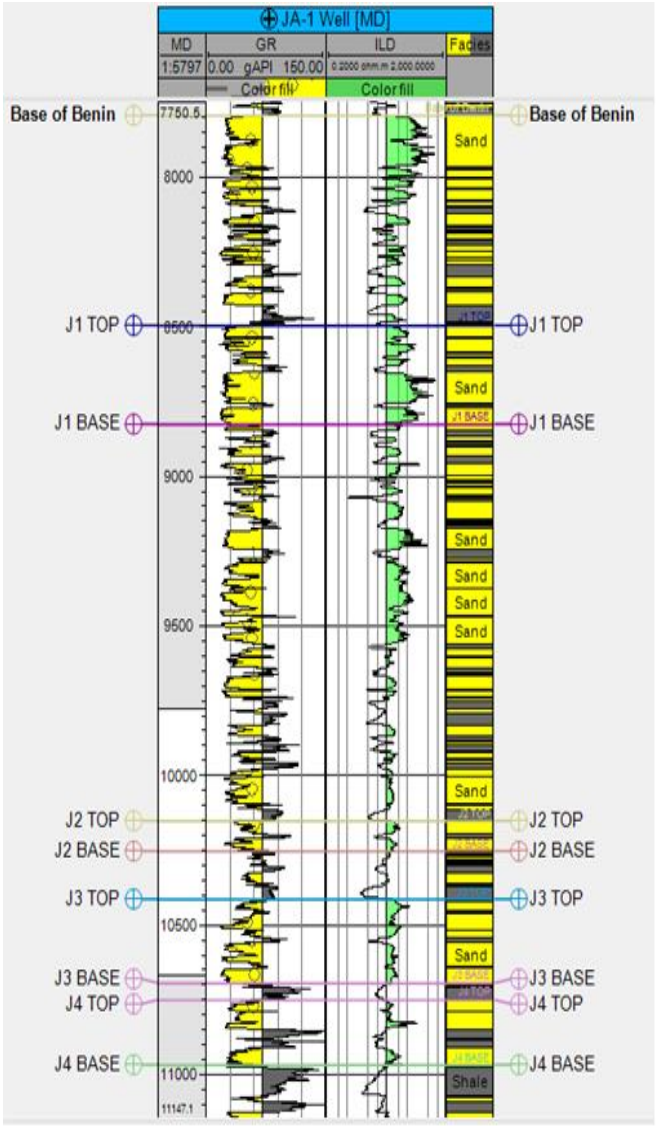

Fig 6 Reservoir Delineation

➢ *Quantitative Interpretation*

The quantitative interpretations involve the use of mathematical models and relations which establish a congruent link between log responses and formation parameters. Reservoir models were therefore built upon the measurement and derivation of petrophysical parameters which further revealed the petrophysical parameters away from well control. Some of the essential petrophysical parameters calculated for this project include:

- *Volume of Shale*

The calculation of shale volume (Vsh) was executed through an established approach involving in Equation (1) and Equation (2).

$$I_{GR} = \frac{GR\ log - GRmin}{Grmax - GRmin} \quad (1)$$

Where;

I_{GR} is the gamma-ray index, GR_{log} in conjunction with the picked log value, and GR_{min} and GR_{max}, and values from sand and shale baselines.

The second step was to employ Steiber's (1970) Equation. The equation incorporates the result obtained from the IGR above. The formula is stated below:

$$Vsh = \frac{IGR}{3-2\times IGR} \quad (2)$$

Where Vsh is the shale volume

- *Porosity*

Porosity (Ø) represents the void percentage relative to the rock's total volume. Bulk density values from formation density logs are employed within equation (3) to derive porosity below:

$$Ø_{DEN} = \frac{\rho m - \rho b}{(\rho m - \rho f)} \quad (3)$$

Where ρm is matrix density equal to 2.65g/cc, ρb is formation bulk density from density log and ρf is fluid density respectively.

- *Water Saturation*

Water Saturation was calculated using Archie's Equation, which is stated as

$$Sw = \frac{1}{ø} \times \frac{\sqrt[2]{Rw/Ro}}{1} \quad (4)$$

$$\text{Apparent water resistivity (Raw)} = \frac{\Phi^{m}}{a} * Rt \quad (5)$$

Where,
Sw = Water Saturation
Rw = water resistivity
Φt = Total Porosity
a = constant value
Rt = true resistivity
m = constant value

To compute the R_w from the log, a clean water-bearing zone from the log was identified and the resistivity of this zone from a deep resistivity log was recorded.

Where Ro is the formation resistivity of the water zone and Rt is the resistivity of the log reading.

- *Residual Hydrocarbon Saturation*

Residual hydrocarbon saturation (Shr) signifies the hydrocarbon remaining in the flushed zone, calculated as the difference between flushed zone water saturation and unity.

$$S_{hr} = 1-S_{xo} \quad (6)$$

For example, Well JA-1 Reservoir J1, interval of 8494-8826ft with S_{xo}=0.8(80%) has S_{hr} value of 0.2(20%).

- *Movable Hydrocarbon Index (H_{IM})*

This is the ratio of water saturation (Sw) and the flushed zone saturation (Sxo)

Bateman R., (1990). If the ratio Sw/S_{xo} is equal to 1.0 or greater, the hydrocarbon was not moved during the inversion. Whenever Sw/Sxo is less than 0.7 for sandstone or less than 0.6 for carbonate, movable hydrocarbons are indicated. (Schlumberger 1972)

$$H_{IM} = \frac{Sw}{Sxo} \quad (7)$$

- *Hydrocarbon Saturation*

Hydrocarbon Saturation, Sh is the percentage of pore volume in a formation occupied by hydrocarbon. It can be determined by subtracting the value obtained for water saturation from 100% i.e.

$$S_H = (100 - S_W)\ \% \quad (8)$$

- *Permeability (K)*

Permeability is the ability of a rock layer to transmit fluids, such as oil, gas, and water. It measured in (mD) millidarcy. The permeability was gotten from Schlumberger Equation for estimating permeability. This is stated as:

$$Phie = (1-Vsh) * \Phi \quad (9)$$

Where Phie (Φe) is the effective porosity

$$\text{Formation factor (F)} = 1 / (Phie\ \hat{}\ 2) \quad (10)$$

Irreducible water saturation (Swirr): (F /2000) ^ 0.5 (2.11)

$$\text{Permeability(K)} = 10000x\frac{\phi e\hat{}4.5}{Swirr\hat{}2} \quad (12)$$

$$Swirr = \sqrt{\frac{F}{2000}} \quad (13)$$

Where Swirr is the irreducible water saturation

➢ *Data Processing and Interpretation*

- *Lithological Identification in 'OY'-Field*

JA-1 Well (Figure 5) extends from 500–12979.6ft and penetrates several sand beds interbedded with shale. On the gamma-ray log, the lithology in yellow and gray denote sand and shale respectively. The most productive sand bed in the well is the Sand J1 because of its high porosity and permeability values (24% and 1804mD respectively).

- *Reservoir Delineation*

The gamma-ray log from the wells is shown side by side with their deep resistivity log used to delineate reservoirs in the well. Four reservoirs (J1, J2, J3, and J4) were identified and analyzed as potential hydrocarbon reservoirs due to high resistivity values (Figure 6).

- *Petrophysical Analysis*

The reservoirs in OY-Field located in the Niger Delta, are represented in a single JA-1 well. The reservoirs were delineated based on log-modified integration of low gamma ray counts with high resistivity was the base of the zoning to determine hydrocarbon-bearing sand. A density log was

used to analyze the porosity; fluid type cannot be discriminated due to the absence of a Neutron log. The JA-1 well penetrated through 12979.6ft (3879.4m) with reservoir sands J1, J2, J3, and J4 respectively were found within this interval (Table 2). The analysis shown in Table 2 was based on the cutoff average for water saturation, porosity, and lithology of 0.6, 0.15, and 0.5 respectively.

Table 2 Average Petrophysical Parameter of the Reservoir Sands in JA-1 well

RESERVOIR	Top (Ft)	Base (Ft)	Net Pay	NTG (Ave)	Ø%	Sw_(Ave)	Sh_(Ave)
J1	8494	8826	209	0.89	0.24	0.37	0.63
J2	10152	10252	57	0.80	0.21	0.55	0.45
J3	10412	10693	114	0.86	0.22	0.53	0.47
J4	10749	10975	91	0.86	0.16	0.64	0.36

III. SEISMIC ANALYSIS

➢ *Well Tie to Seismic*

The well-to-seismic correlation was established utilizing data from the JA-1 well, combined with a check-shot survey to create a synthetic seismogram for aligning with the field's seismic data (as depicted in Figure 7). A harmonious match between the synthetic and seismic data was achieved following a 20ms bulk shift.

➢ *Seismic Structural Interpretation*

- *Horizon Mapping*

Horizon interpretation was carried out using synthetic processing on both inline and cross-line seismic data. Significant seismic reflections, indicative of the uppermost points of the main reservoir sands, were pinpointed in the seismic data for the purpose of mapping (see Figure 8). Database and polarity critically determine seismic character. The face and polarity of seismic data are zero phases of European polarity, where the trough is blue and the beak is red. The over-red character depicts low impedance and is contemporaneous with a prospective reservoir of younger sediment where the Niger Delta belongs.

- *Fault Interpretation*

The interpreted seismic sections revealed two (2) faults, one being major and the other minor fault was mapped on seismic sections over the entire field (Figure 9a). One major listric normal fault (F1) was mapped with one minor fault (F2) which had a relatively NE-SW trend and dip southwest, the fault was modeled for the enhancement of the orientation (Figure 9b). The major characteristics of the listric fault were apparent on the field (seismic section) especially the thicker strata when the hanging wall block of the listric fault is drawn left from the footwall block under extensional force which is a result of ongoing or continuous sedimentation. They are excellent targets for hydrocarbon accumulations.

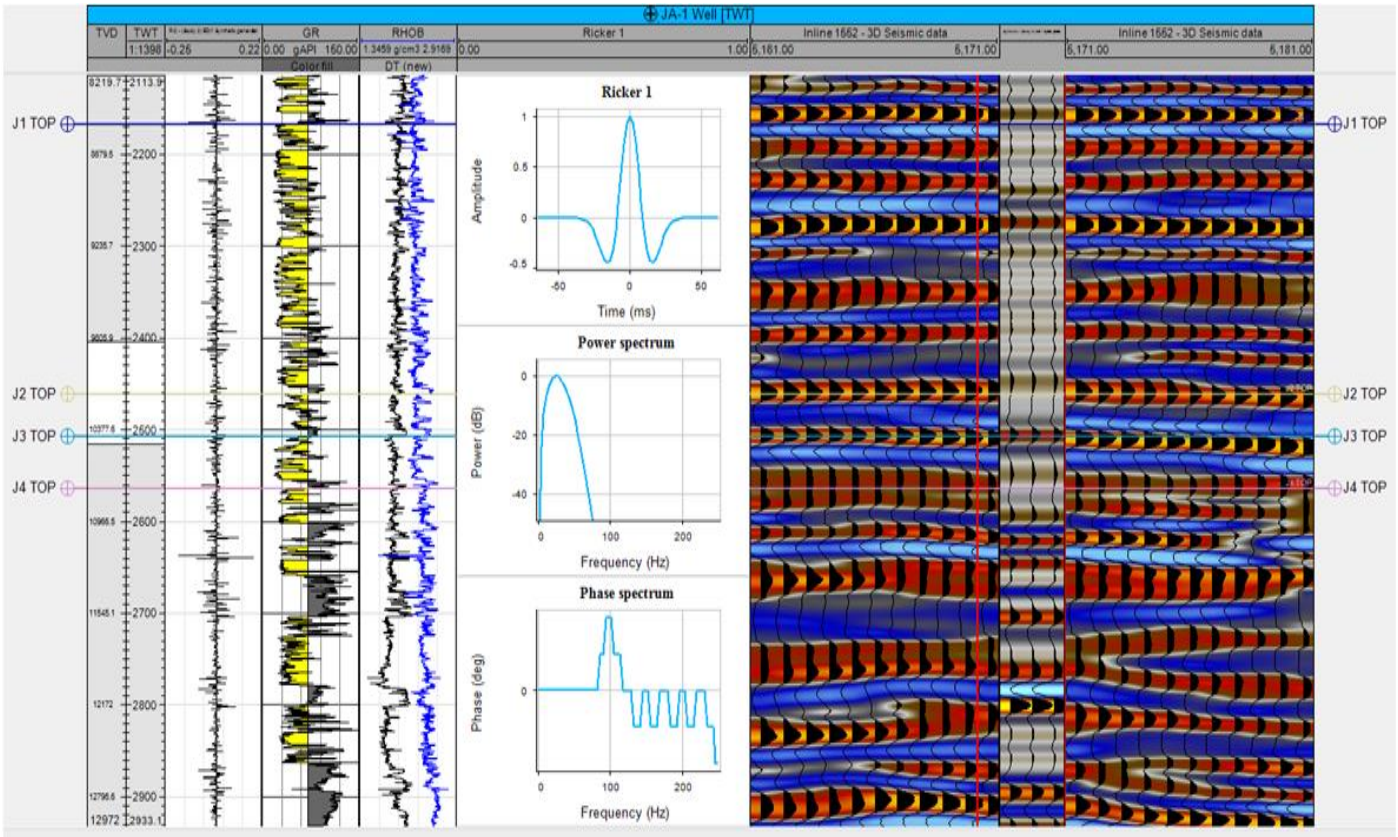

Fig 7 Well to Seismic Tie

ISSN No:-2456-2165

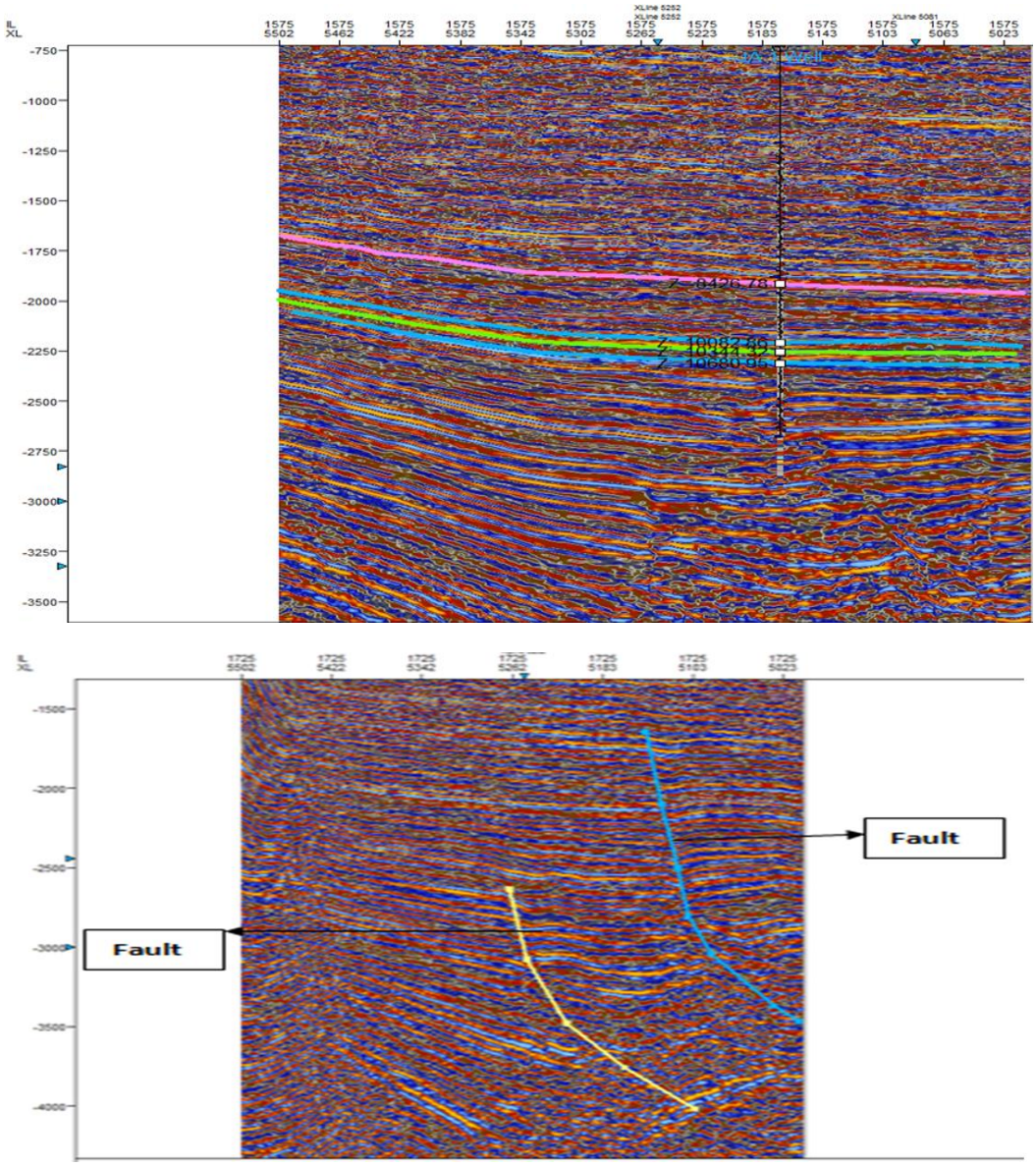

Fig 8 Horizon Interpretation

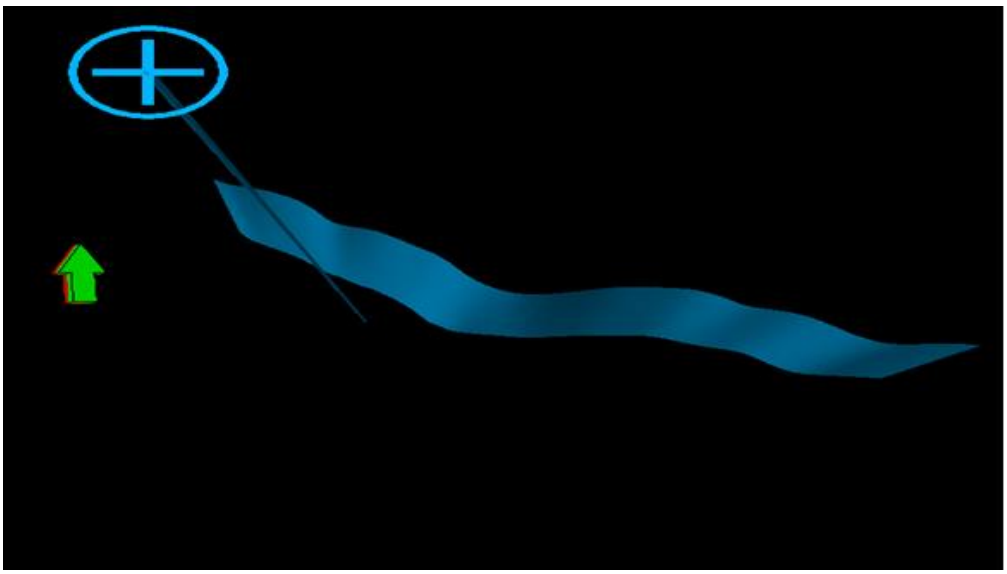

Fig 9a-b: Seismic section displays the Major and the Minor Listric normal Fault Interpretation (b) Minor Listric normal Fault Modeling with Well.

ISSN No:-2456-2165

- *Time and Depth Maps*

Four horizons were delineated on both the well logs and seismic section also four were mapped all through the study area. Structural time maps and depth maps were generated at the top of four reservoirs. This was done in other to delineate the orientation of the fault and zone of structural high and low. The effectiveness of sealing is not influenced by the quantity of throws or the presence of shale/clay distributed along fault planes (Bush, 1975; Weber and Daukoru, 1975). Weber and Daukoru (1975) propose that fault sealing can occur when the throws are below 492 feet (150m) or when the proportion of shale/clay present along the fault plane exceeds 25%. Horizon J1, J2, J3, and J4 time structure maps were generated (Figure 10a-d) with check-shot function (Figure 11) the depth structural maps for the four horizons were generated are presented in a map function window (Figure 12a-d) which uses color to represent structural features. The map shows clearly the orientation of the major fault. The structural high is observed in the Northeast part of the survey area while the structural moderate is observed in the South part and low in the Southwest part of the survey.

All horizon time and depth structural map was observed and show that the same feature is present in the entire horizon. The structural highs were still present at almost the same position on the entire horizon.

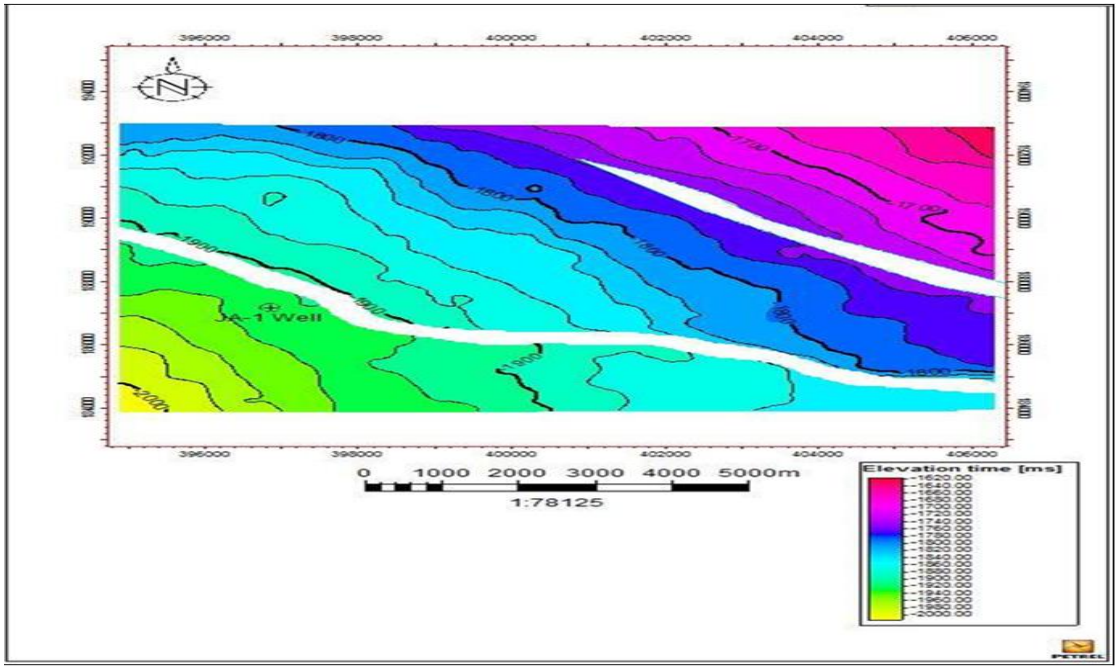

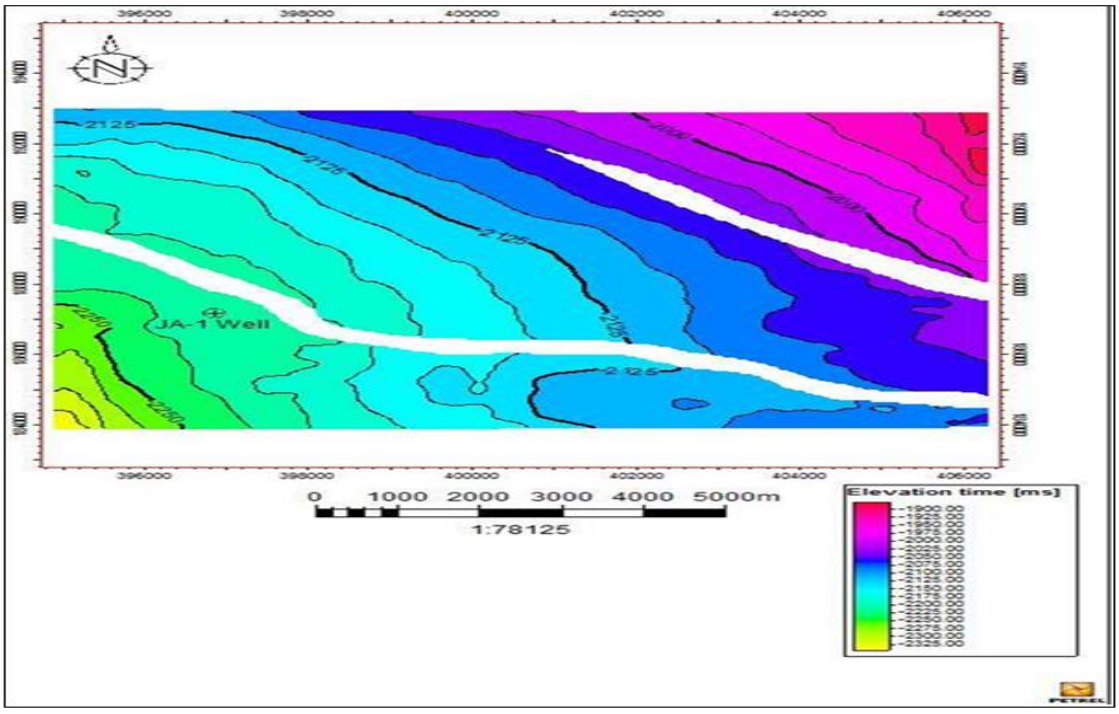

ISSN No:-2456-2165

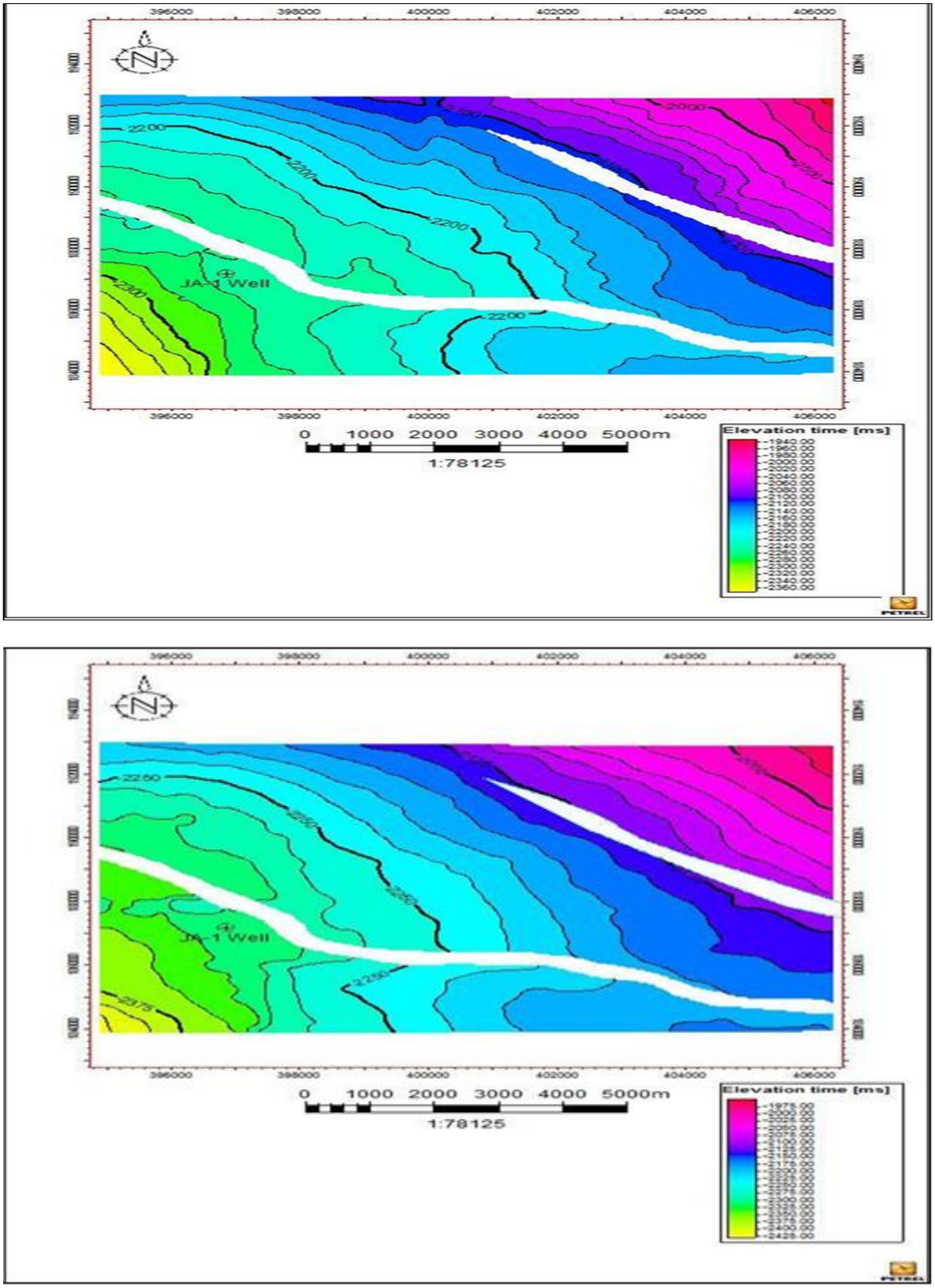

Fig 10a-d: Structural Time Map for Reservoir J1, J2, J3 and J4.

ISSN No:-2456-2165

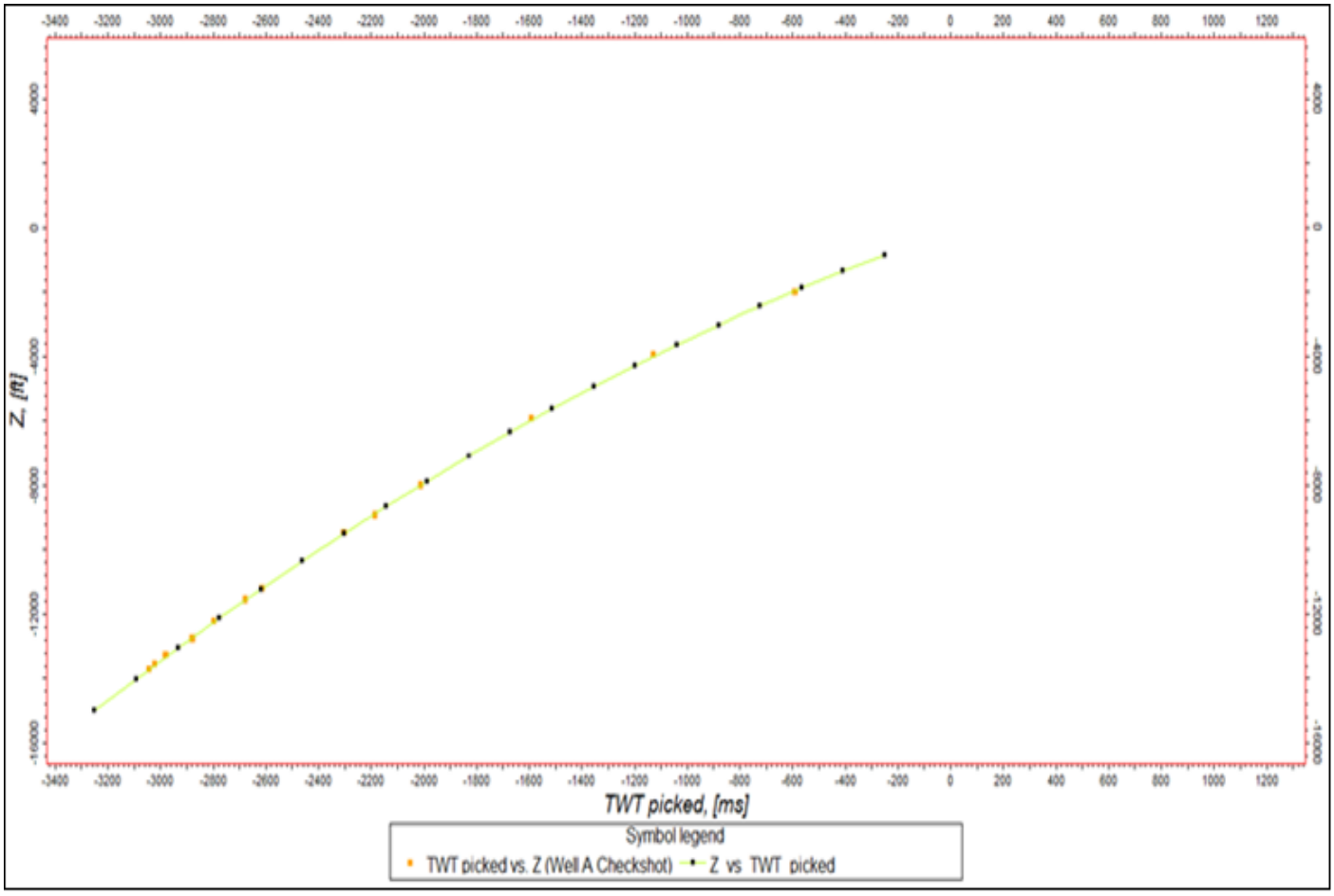

Fig 11 Time-Depth Conversion Polynomial Fitting

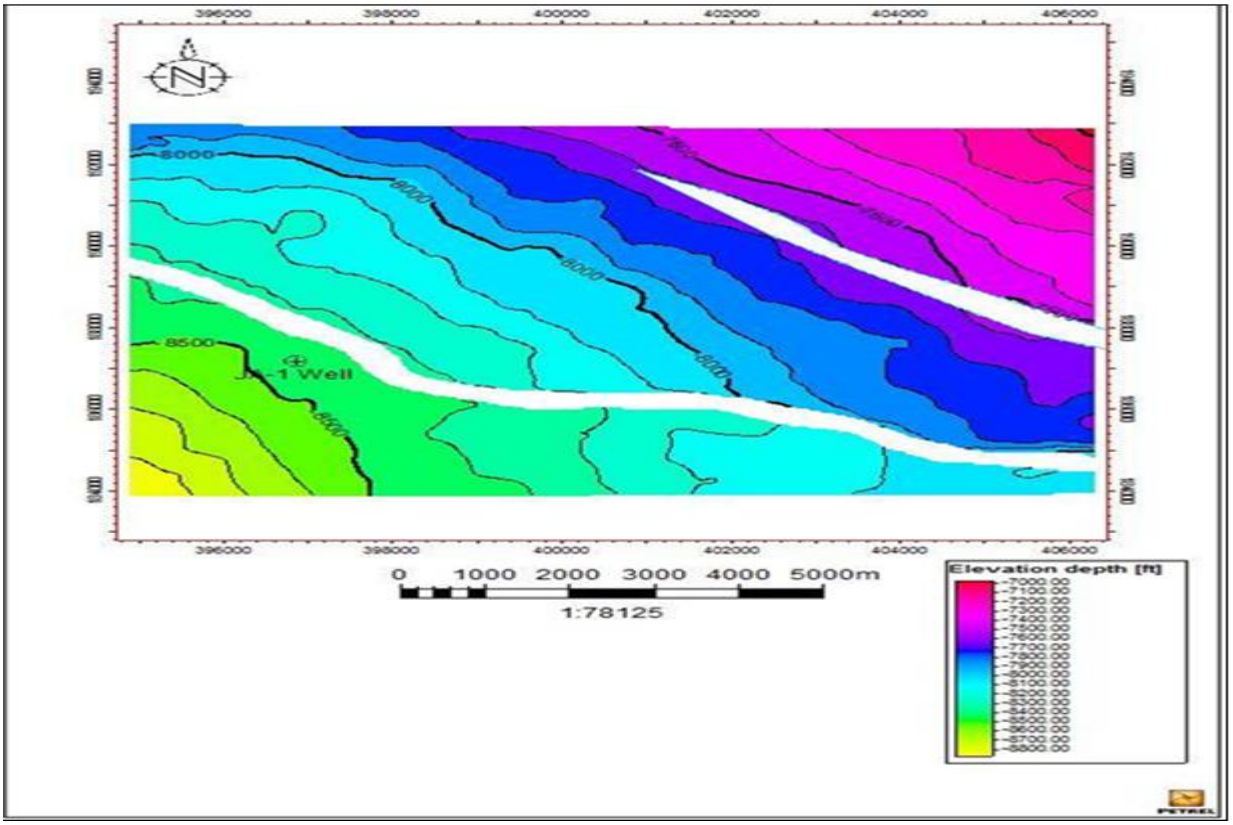

ISSN No:-2456-2165

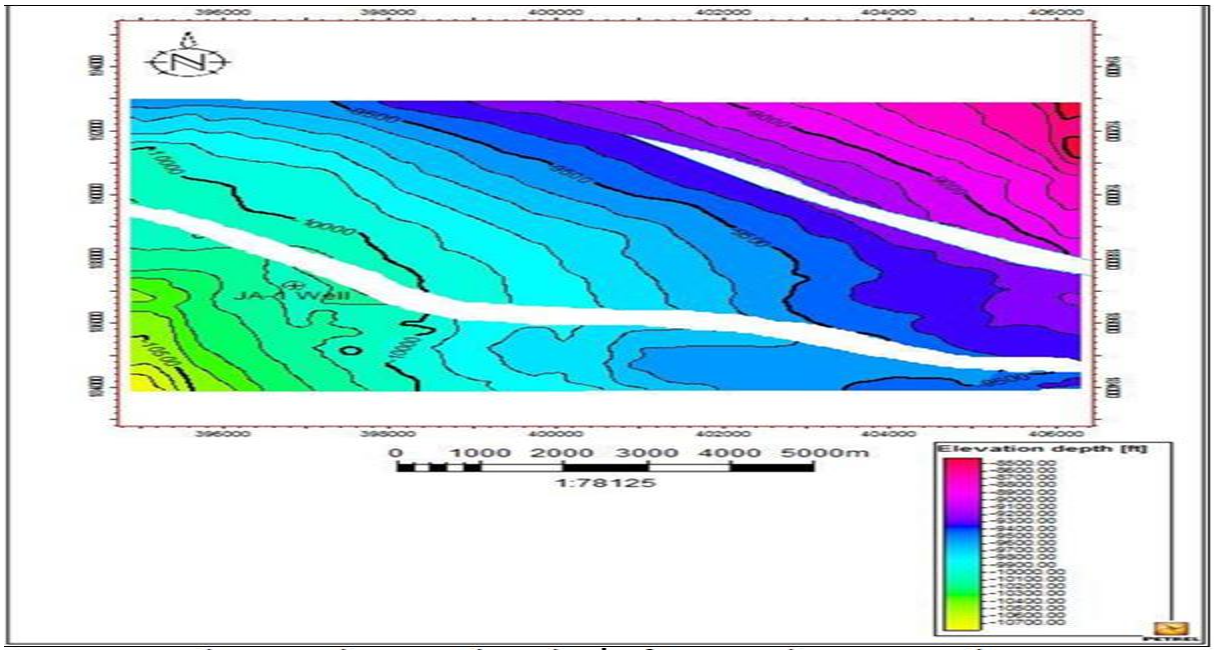

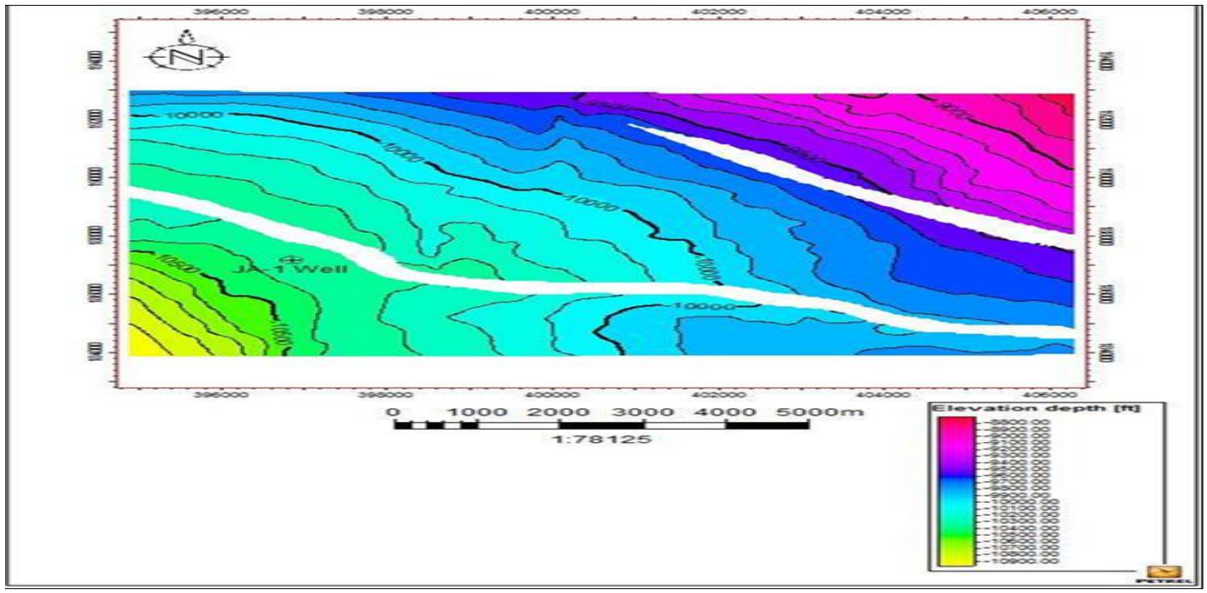

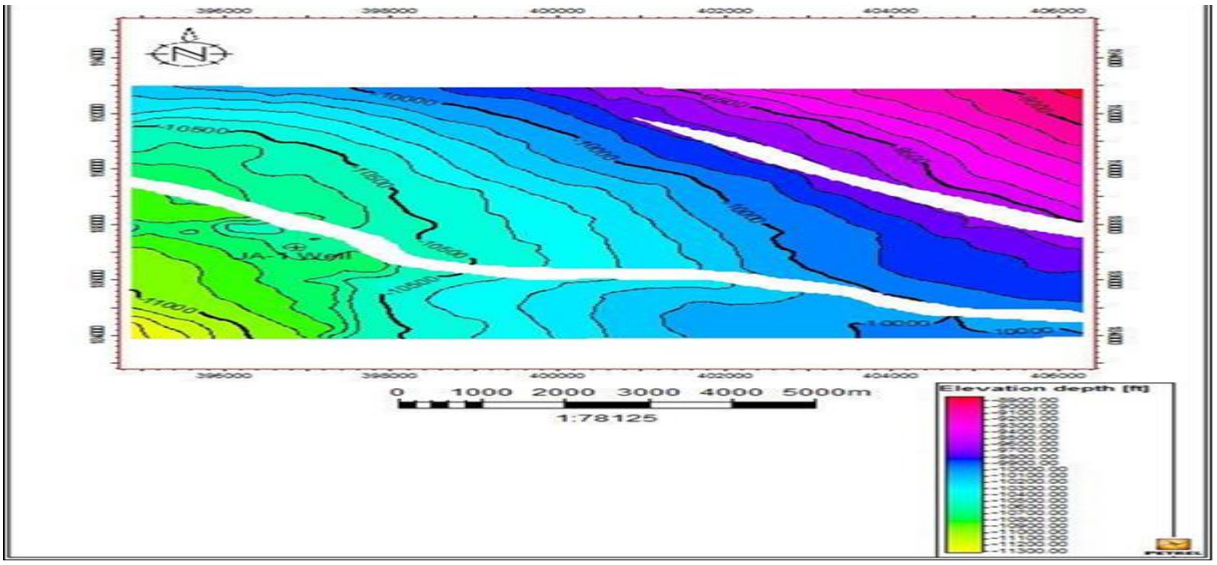

Fig 12a-d: Structural Depth Map for Reservoir J1, J2, J3 and J4

ISSN No:-2456-2165

- *Seismic Attribute*

To gain deeper insights into reservoir characteristics, extent, and the influence of hydrocarbon fluids on seismic responses, RMS amplitude, Extra value, and Minimum amplitude of seismic attributes were computed for the well. These attributes are depicted in Figures 13a, 13b, and 13c, respectively. By validating attribute outcomes with existing well data, a novel prospect emerged. This prospect was identified using a cross-plot of Extra value against Minimum amplitude, as illustrated in Figure 14. Furthermore, the RMS signature indicated enhanced hydrocarbon-bearing potential within sand layers.

- *Static Geological Model*

Creation of Static Geological Model: In the pursuit of dynamic simulation and comprehensive well and production performance evaluations, the construction of an accurate static model became crucial. This model aimed to faithfully represent the subsurface reality of sand layers J1, J2, J3, and J4 encountered in the JA-1 well. The static geological model, illustrated in Figure 15, was developed by amalgamating pertinent subsurface data and interpretations from preceding sections. The model's foundation included 3D seismic structural interpretation, lithological descriptions, facies interpretations, as well as porosity, permeability, and initial water saturation values derived from log analyses. The static model was structured with a 20-cell grid layering, as shown in Figure 16. For the petrophysical properties model encompassing net-to-gross ratio, porosity, permeability, and water saturation distribution values, a Sequential Random Function Simulation (SRFS) method was employed. Concurrently, Sequential Indicator Simulation (SIS) was used to determine facies distribution, particularly for Sand layers J1 to J4. The results of these stochastic techniques are visualized in Figures 17a through 17f.

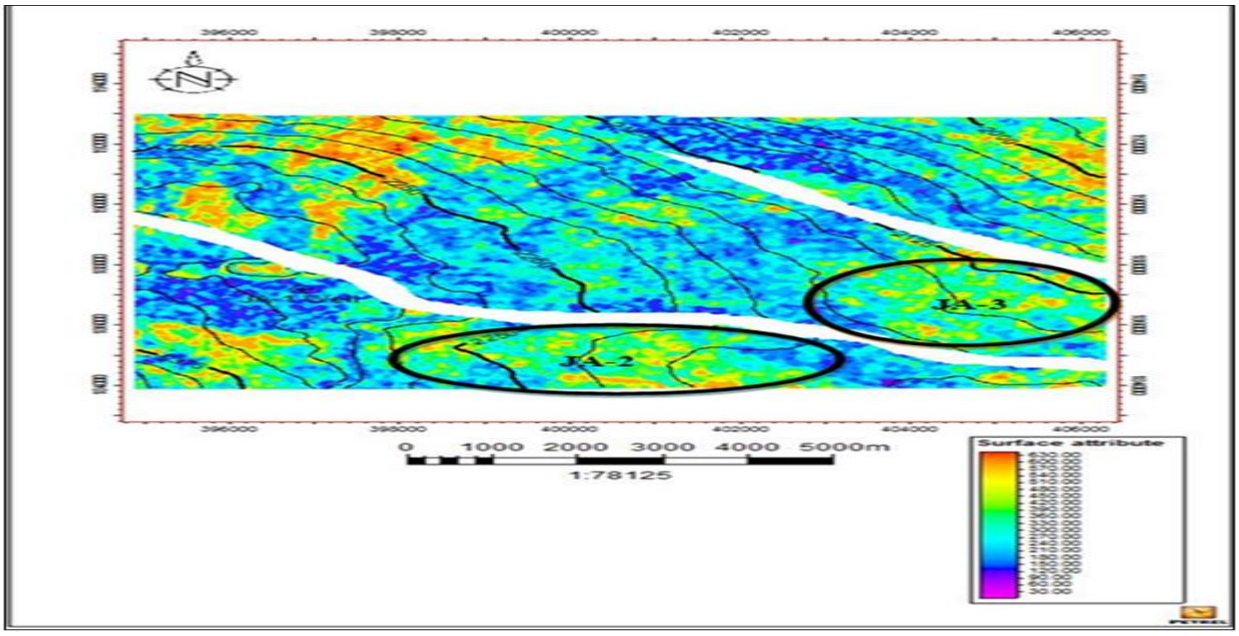

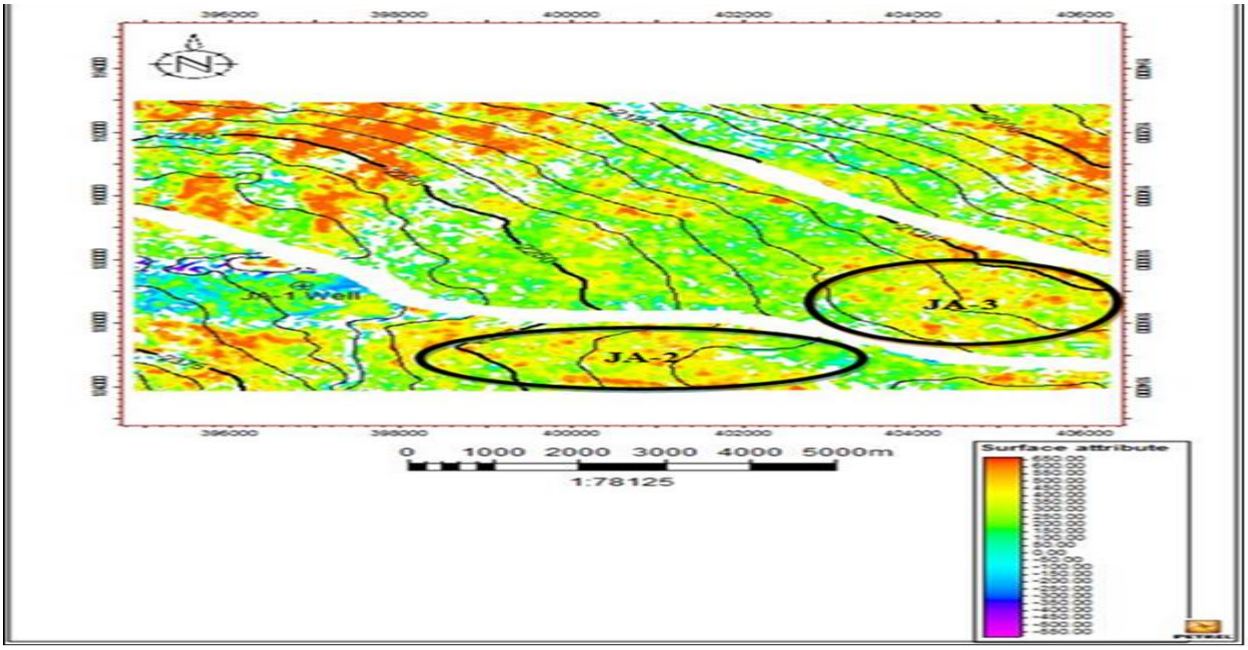

ISSN No:-2456-2165

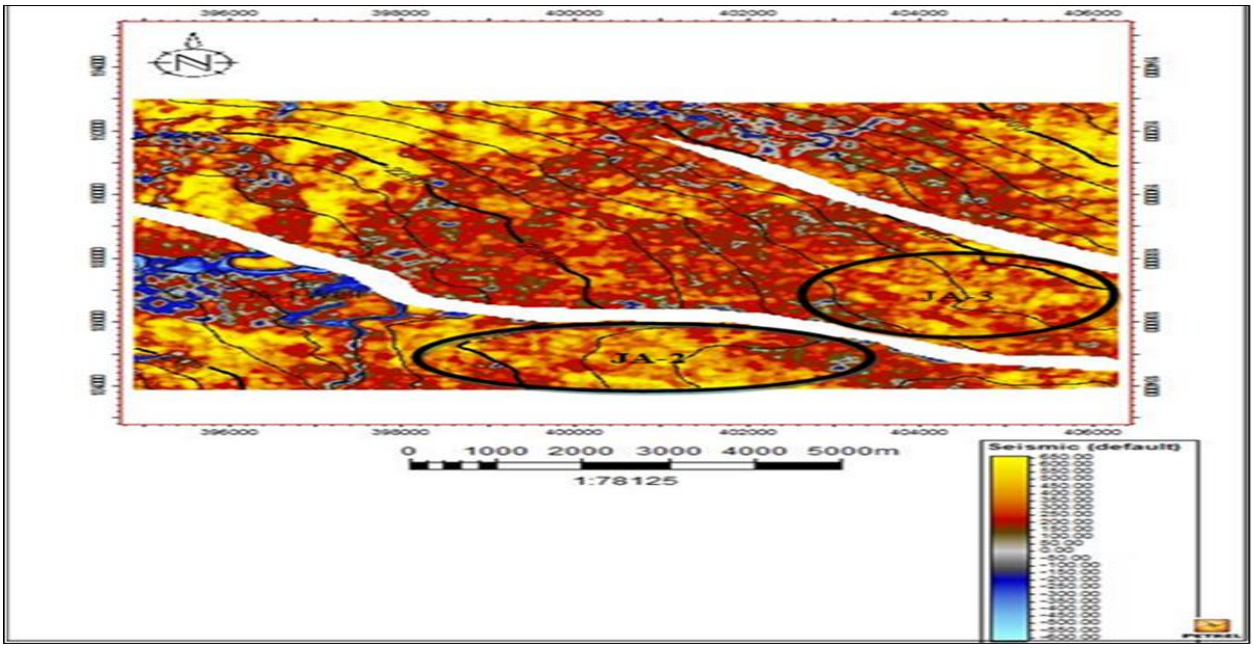

Fig 13a-c: RMS amplitude, Minimum amplitude, and Extra value Map with well and New Prospects JA-2 and JA-3

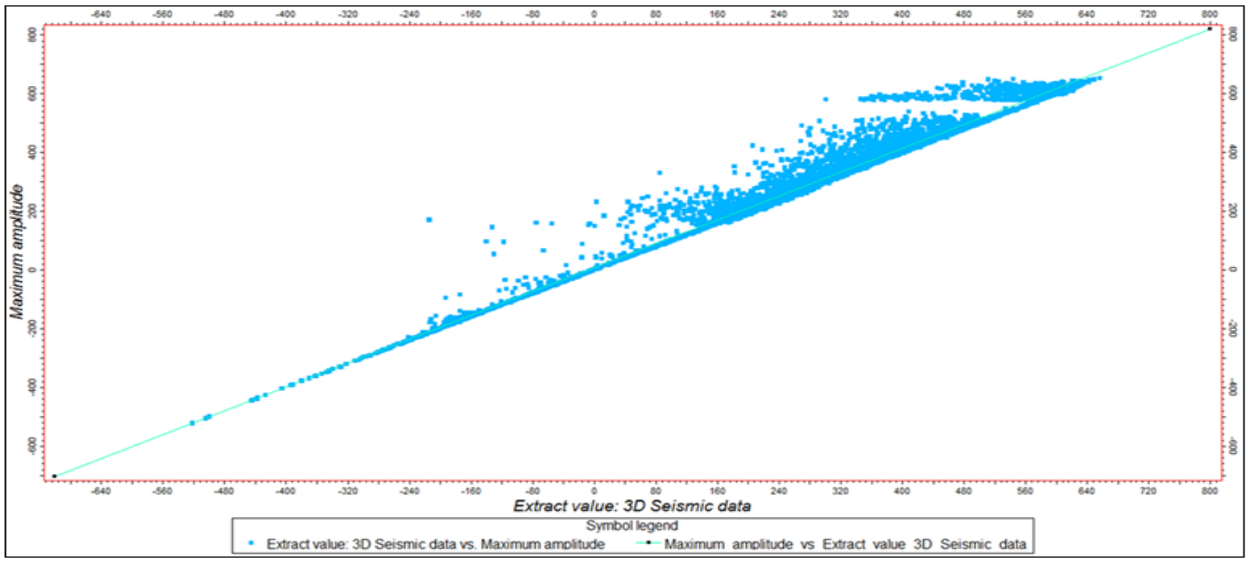

Fig 14: Cross-plot of Maximum Amplitude and Extract value

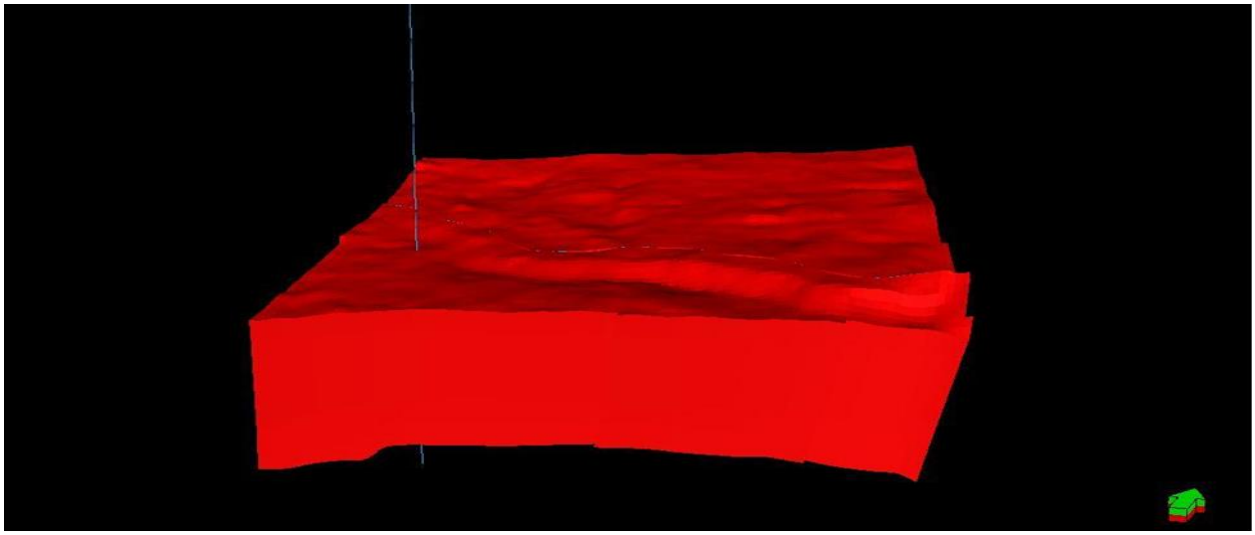

Fig 15: The Static Geological Model of Sand J1 to J4 of the Entire JA-1 well

ISSN No:-2456-2165

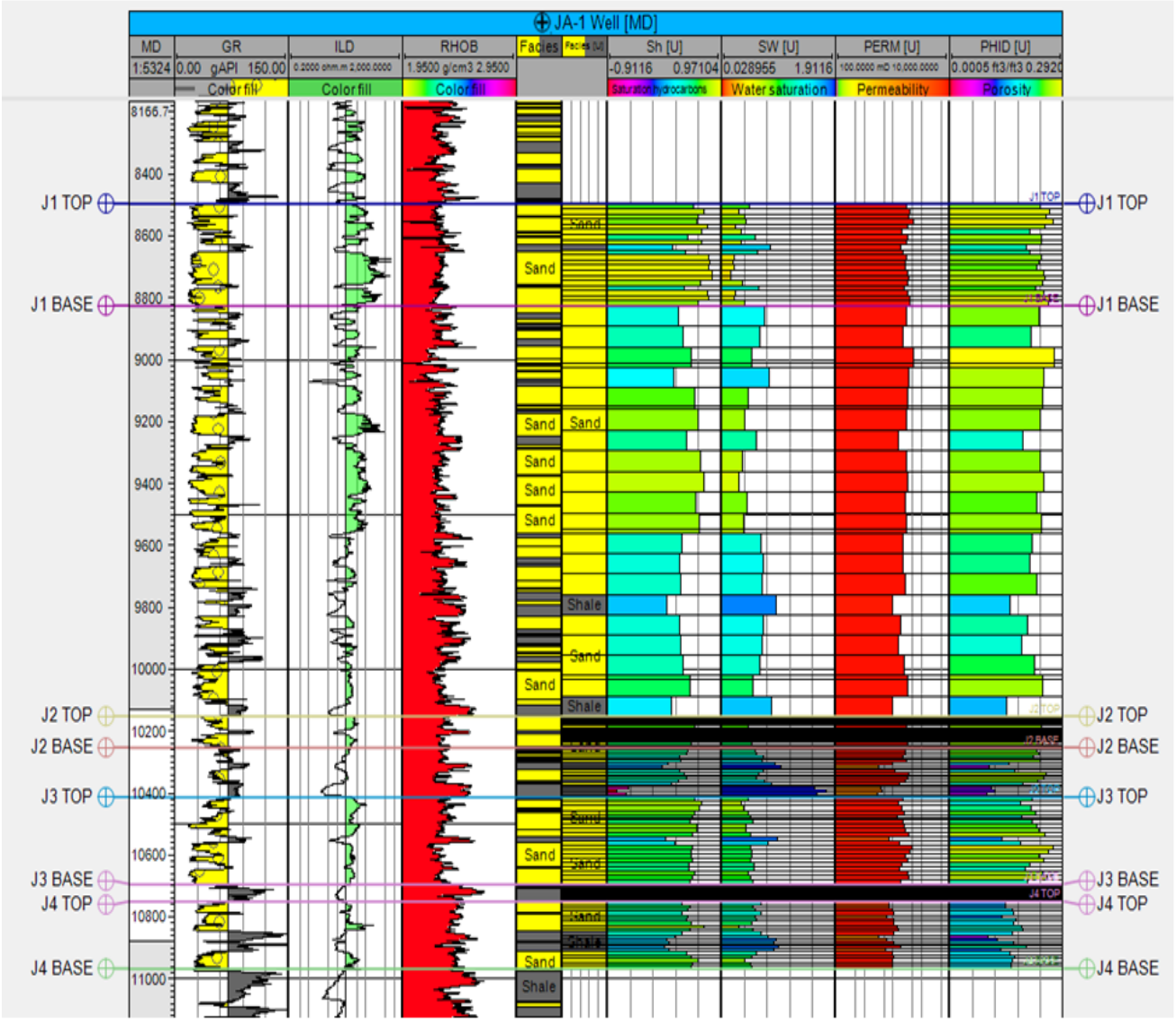

Fig 16: Facie, Hydrocarbon Saturation, Water Saturation, Permeability, and Porosity Property Distribution in sands J1, J2, J3 and J4

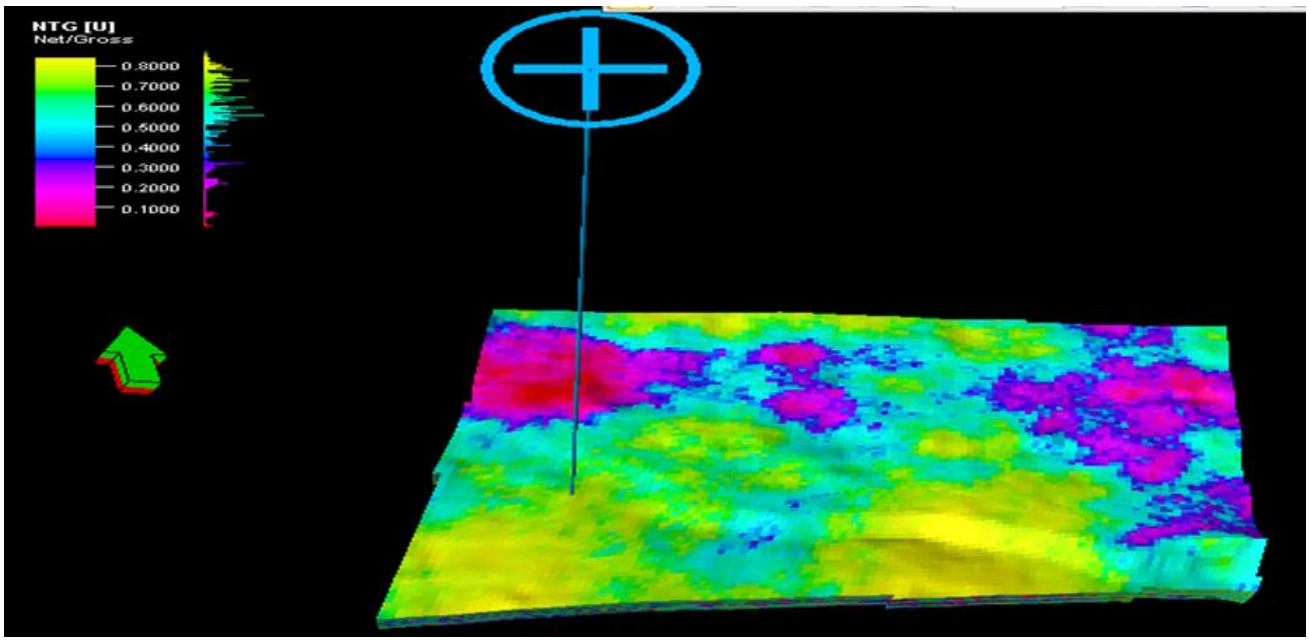

Fig 17a: Net to Gross Model

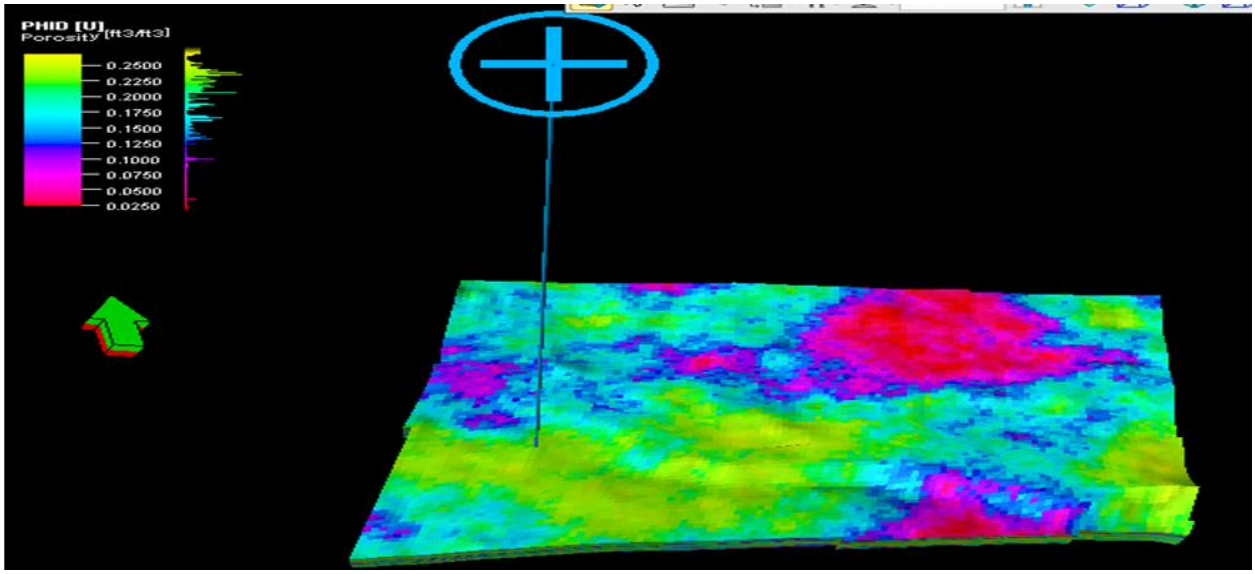

Fig 17b: Porosity Model

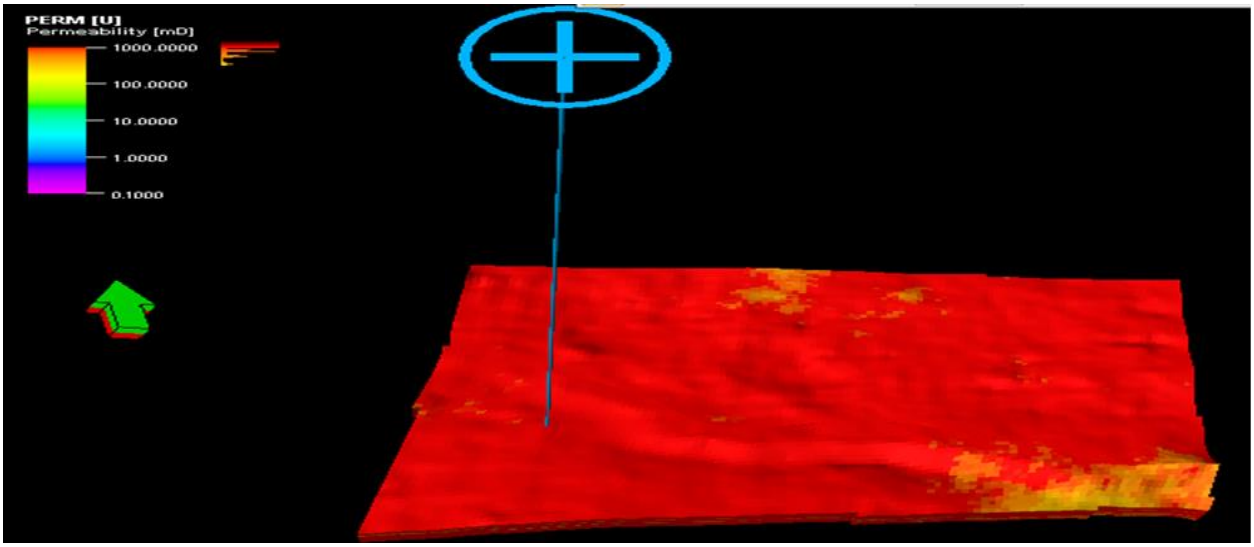

Fig 17c: Permeability Model

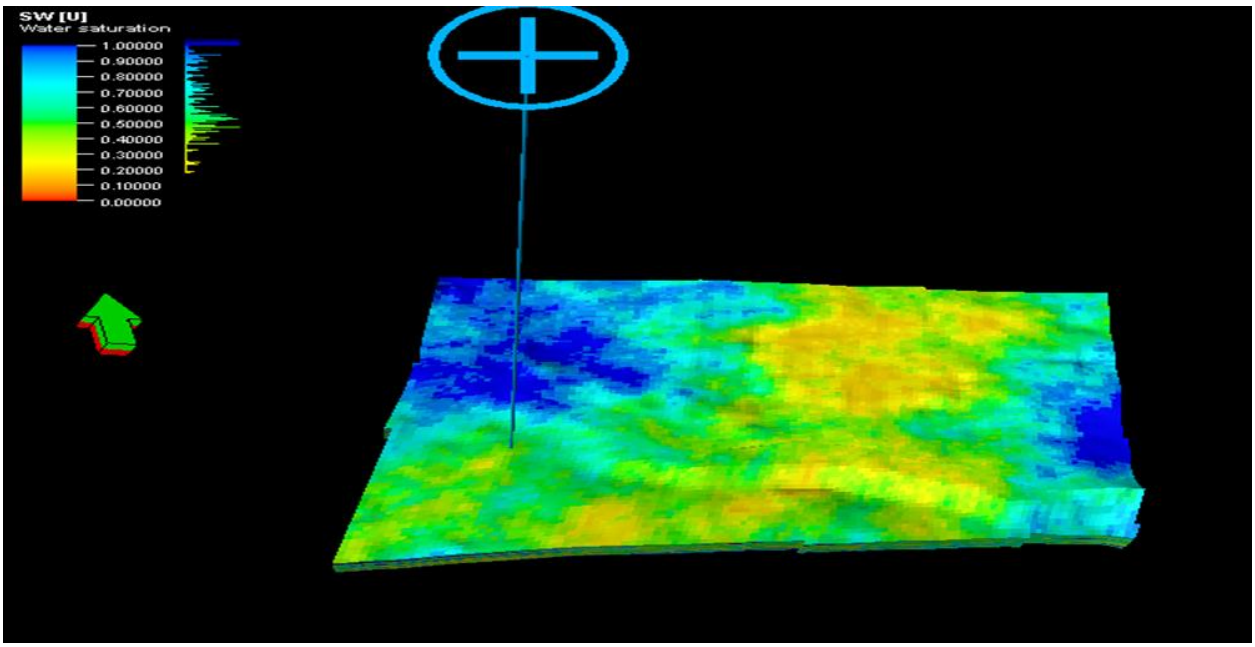

Fig 17d: Water Saturation Model

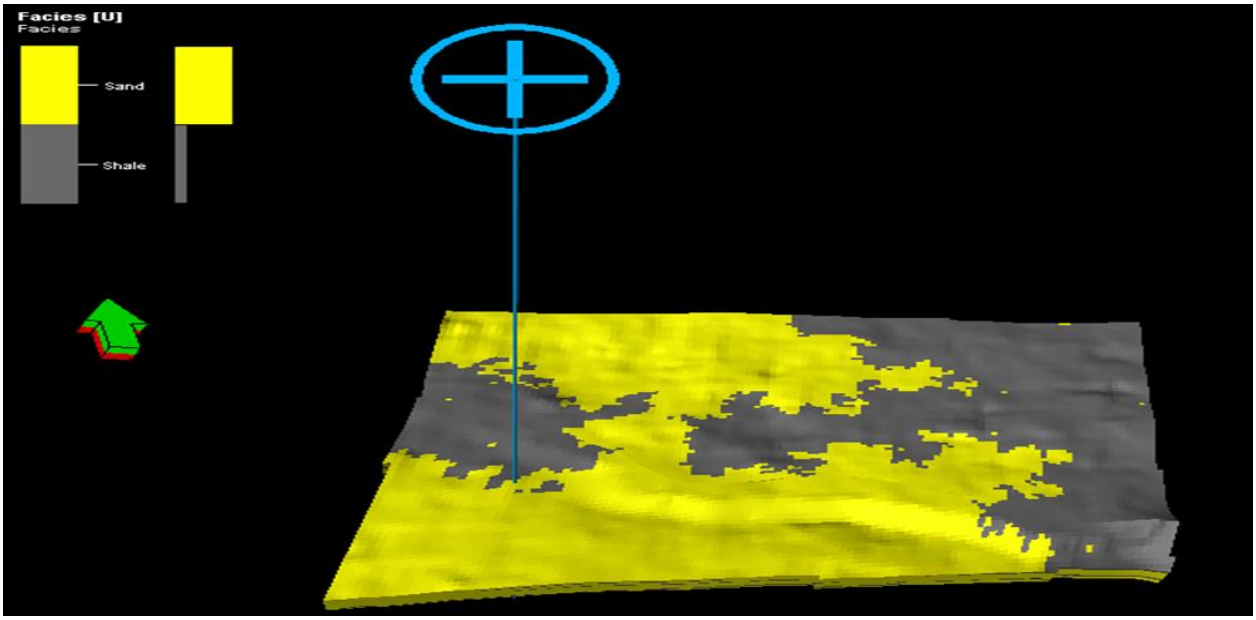

Fig 17e: Facies Model

IV. RESULT AND DISCUSSIONS

➢ *Structural Interpretation of Study Area*

Geologically, the study area stands out as a distinct domain characterized by a prevalence of fault-related structural formations. This structural configuration gives rise to a notable potential for fault-assisted processes. A dominant influence on deposition is attributed to the significant presence of listric normal faults, a salient feature extracted from the 3D data utilized.

The field's structural makeup takes the form of an elongated anticline, confined within the expanse defined by the major structure-building fault trending in a west-southeast direction to the north – acting as the principal zone of displacement. Two particular faults stand out, terminating at the field's northwest fringes. As the structure extends eastward, it culminates in the elevation of the highest points found in the majority of the reservoirs encountered across the field's drilled wells. Within the field, the landscape is marked by the presence of numerous synthetic and antithetic faults. These smaller-scale intra-field faults exhibit varying lengths, with many closely aligning parallel to the major structure-building fault bounding the northern perimeter.

➢ *Petrophysical Characterization of the Reservoirs*

The reservoir sand thickness for the well ranges from (281Ft-332Ft). The sand displays remarkable porosity and permeability characteristics, facilitating efficient fluid storage and transmission. Hydrocarbon occurs at four intervals in an appreciable high ratio in reservoir sand except for reservoir sand J4 has been on the list.

- *The volume of Shale (Vcl):*

This determines how clear the reservoir sand is, also the type of equation to be used for shaly-sand analysis. The reservoir sand in this well is relatively clean with shale content which averages at 11%,20%,16%, and 17% respectively shown in **(**Table 1).

- *Porosity:*

In the reservoir sands throughout the wells, generally, the porosity values are fairly high with an average of 22%, 24%, 21%, and 16% in the reservoir respectively. They are very good porosity values are owed to the low shale content shown in **(**Table 1).

- *Water Saturation:*

Within the well, water saturation exhibits a range from 37% to 64%. Notably, reservoir pore spaces typically accommodate a mixture of hydrocarbon and water. A low water saturation accompanied by a high porosity interval signifies a higher presence of hydrocarbons, and conversely, a high-water saturation implies a lower hydrocarbon presence, as presented in (Table 1).

- *Permeability:*

The permeability for all reservoirs is very high. Reservoir J1 has the highest permeability across the reservoirs with permeability values ranging from 1803 to 988mD shown in **(**Table 1).

- *Net Pay Assessment:*

Among the sand layers, Sand J1 emerges as the most promising with an impressive net pay of approximately 209 feet and a considerable hydrocarbon saturation of around 63%. This is closely followed in potential by J3, J2, and J4 in descending order, as detailed in Table 1**.**

➢ *Seismic Attribute*

RMS amplitude, Extra value, and Maximum amplitude of seismic attribute were generated within the well in OY-field, to be able to acquire better information around the well and to find the extent of prospect that indicates the hydrocarbon target shown in (Figure 13a-c). New prospect JA-2 and JA-3 was proposed as a result of the attribute generated showing better sand hydrocarbon bearing which are validated from the cross plot shown in (Figure 14).

➢ *Static Modeling*

- *Sands' Structural Representation*

As depicted in (Figure 9b), the structural model highlights a system of Listric normal faults. Among these, a significant Listric fault stands out, characterized by a southwestward dip. This fault holds a substantial extent and reinforces the findings derived from the depth structure map.

- *NTG Distribution Map*

(Shown in Figure 17a) illustrates favorable net-to-gross ratios ranging from 0.6 to 0.8 within both the OY field's well area and the nearby prospective region. In contrast, areas situated farther from the well exhibit lower net-to-gross ratios, indicating reduced reservoir quality.

- *Porosity Distribution Map*

Presented in a 3D perspective in (Figure 17b), the porosity model map highlights the prevalence of sound porosity levels (ranging from 0.24 to 0.16) within the OY field's well area and the adjacent prospective zone. This distribution signifies that there is ample pore space available to accommodate fluid movement.

- *Permeability Distribution Map*

The 3D perspective view of the permeability model map, depicted in (Figure 17c), underscores noteworthy permeability values ranging from 1803 mD to 988 mD within both the OY field's well area and the prospective region. These values reflect strong interconnectivity among the pore spaces within the sand of the well and prospect areas, facilitating efficient fluid transmission.

- *Water Saturation Distribution Map*

A glimpse into the 3D perspective of the water saturation model map reveals varying water saturation levels within the OY field's well area, ranging from 0.35 to 0.65. This variation indicates a region of moderate hydrocarbon presence. Conversely, regions farther from the well exhibit higher water saturation levels exceeding 0.75 (Figure 17d).

- *Facies Distribution Map*

The facies model map, presented in a 3D perspective and shown in (Figure 17e), showcases the presence of moderate to good reservoir sand within the OY field's well area. The regional depositional trend is assumed to follow an NW-SE direction.

V. CONCLUSION

The outcomes and insights detailed within this study construct the fundamental structural framework for a comprehensive model employed in modeling reservoir properties and simulating fluid flow within the reservoir. Establishing a robust and all-encompassing model holds paramount importance in modeling endeavors, serving to comprehend and mitigate potential risks, while also proving instrumental in assessing induced seismic hazards. A thorough petrophysical evaluation of the JA-1 well yields a predominant reservoir presence spanning the entire field. Particularly promising is the J1 sand reservoir, characterized by its noteworthy porosity values ranging from moderate to very good, accompanied by low water saturation, high hydrocarbon saturation (Sh), minimal residual hydrocarbon saturation (Shr), low hydrocarbon movability index (Sw/Sxo < 0.7), significant permeability, and a moderate to good net-to-gross ratio. Encouragingly, the J1 horizon signifies a substantial accumulation of hydrocarbons in economically viable quantities. The underlying accumulation and retention of hydrocarbons within the field stem from its structural configuration, heavily influenced by a fault-closed dominated interplay, shaped by faulting. Faults are pivotal in the trapping process, and their interplay is influenced by discrete and continuous attributes. These characteristics provide insights into observed facies properties and offer valuable information about petrophysical parameters like net-to-gross ratio, porosity, water saturation, and permeability. Facies examination notably discloses the presence of moderate to high-quality sand within the J1 reservoir, congruent with its petrophysical attributes. The application of 3-D Static Modeling to the OY field has greatly enhanced our spatial comprehension of both discrete and continuous properties across the field. Consequently, this research has established a geological model for the OY field, capable of being updated with emerging data to bolster ongoing field development efforts. This model holds potential utility for reservoir engineers, serving as a reliable resource during simulation processes. However, to further refine reservoir understanding and robustly interpret depositional environments, it is recommended to incorporate Geochemical and Biostratigraphic studies. In addition, fault seal analysis should be conducted to assess the efficacy of the main fault as a significant trapping mechanism. The utilization of seismic data within the field should encompass the study of minor faults for a comprehensive understanding. Exploring new prospective areas through drilling can provide support to the initial well, enhancing production outcomes. Moreover, generating Neutron log data is advisable to gain deeper insights into fluid content characteristics.

REFERENCES

[1]. **Adiela, U. P**, (2016), Reservoir Characterization of X-Field, Onshore, Niger Delta.*Volume-II, Issue-II, March 2016, pp. 83-89*

[2]. **Stacher, P.,** (1995). Present understanding of the Niger Delta hydrocarbon habitat, in, Oti, M.N., and Postma, G., eds., Geology of Deltas: Rotterdam, A.A. Balkema, p. 257-267.

[3]. **Avbovbo**, A.A, (1978). Tertiary lithostratigraphy of Niger Delta," *American Association of Petroleum Geologists Bulletin*, vol. 62, pp. 295-300.

[4]. **Doust, H**., and **Omatsola, E**. (1990), Niger delta: in J. D. Edwards and P.A. Santogrossi, eds., Divergent/passive margin basins: AAPG Memoir 48, p. 239-248.

[5]. **Bush,** (1975). Fault Sealing Properties. In: **A.Weber, K. J., And E. Daukoru**, (1975). Petroleum Geology of The Niger Delta: 9th World Petroleum Congress, Tokyo, Proceedings, 2: 209-221.Cambridge University Press. Cambridge, UK

[6]. **Knox, G.J**. and **Omatsola, E.M**. (1989) Development of the Cenozoic Niger Delta in terms of the "Escalator Regression" Model and Impact on Hydrocarbon Distribution. In: van der Linden, W.J.M., et al., eds., Proceedings of KNGMG Symposium on Coastal Lowlands, Geology, Geotechnology, Kluwer Academic Publishers, Dordrecht, 181-202.

[7]. **Weber, K. J**. and **Daukoru, E. M**., (1975), Petroleum Geology of Niger Delta: Proceeding of the ninth world Petroleum Congress, volume 2, Geology: London, Applied Science Publishers, Ltd.